0026-895X/06/7001-90–100
MOLECULAR PHARMACOLOGY
U.S. Government work not protected by U.S. copyright
Mol Pharmacol 70:90–100, 2006

Vol. 70, No. 1
21394/3121487
Printed in U.S.A.

Phosducin and Phosducin-like Protein Attenuate G-Protein-Coupled Receptor-Mediated Inhibition of Voltage-Gated Calcium Channels in Rat Sympathetic Neurons

John G. Partridge,[1] Henry L. Puhl III, and Stephen R. Ikeda

Laboratory of Molecular Physiology, Section on Transmitter Signaling, National Institute on Alcohol Abuse and Alcoholism, National Institutes of Health, Bethesda, Maryland

Received December 1, 2005; accepted April 11, 2006

ABSTRACT

Phosducin (PDC) has been shown in structural and biochemical experiments to bind the Gβγ subunit of heterotrimeric G-proteins. A proposed function of PDC and phosducin-like protein (PDCL) is the sequestration of "free" Gβγ from the plasma membrane, thereby terminating signaling by Gβγ. The functional impact of heterologously expressed PDC and PDCL on N-type calcium channel ($Ca_V2.2$) modulation was examined in sympathetic neurons, isolated from rat superior cervical ganglia, using whole-cell voltage clamp. Expression of PDC and PDCL attenuated voltage-dependent inhibition of N-type calcium channels, a Gβγ-dependent process, in a time-dependent fashion. Calcium current inhibition after short-term exposure to norepinephrine was minimally altered by PDC or PDCL expression. However, in the continued presence of norepinephrine, PDC or PDCL relieved calcium channel inhibition compared with control neurons. We observed similar results after activation of heterologously expressed metabotropic glutamate receptors with 100 μM L-glutamate. Neurons expressing PDC or PDCL maintained suppression of inhibition after re-exposure to agonist. Unlike other Gβγ sequestering proteins that abolish the short-term inhibition of Ca^{2+} channels, PDC and PDCL require prolonged agonist exposure before effects on modulation are realized.

G-protein-coupled receptors (GPCRs) are expressed throughout the nervous system and influence systems important for homeostasis. The canonical G-protein signaling pathways consists of a ligand binding to the receptor, exchange of GDP for GTP on the heterotrimeric G-protein α-subunit (Gα), separation of the Gβγ dimer (Gβγ) from the Gα subunit, and modulation of divergent downstream effector proteins by Gα-GTP and Gβγ. For example, free Gβγ can associate with N-type voltage-gated Ca^{2+} channels to reduce the probability of channel opening upon membrane depolarization. The strength and duration of this interaction will be influenced by competition with proteins possessing a high affinity for Gβγ, including Gα-GDP. Therefore, the duration of G-protein signaling is dependent upon the GTP hydrolysis rate because coalescence of the Gαβγ heterotrimer terminates signaling. Other proteins that bind Gβγ with high affinity, such as the carboxyl terminus of GRK2 (ctGRK2) or phospholipase C-β2, attenuate Gβγ signaling (Ford et al., 1998). In this study, we examined how the expression of phosducins, a protein family known to interact with Gβγ, influenced GPCR-mediated N-type Ca^{2+} channel modulation in sympathetic neurons. The goals of the study were 1) to characterize the effects of PDC and PDCL expression within the context of protein-based optical sensor development and 2) to provide insight into possible physiological roles for PDC/PDCL modification of GPCR responses in neurons.

Phosducin (PDC) is a 28-kDa soluble protein expressed primarily in the retina and pineal gland (Schulz, 2001; Sokolov et al., 2004). Retinal PDC has been hypothesized to adjust the gain of luminosity perception in the vertebrate eye (Thulin et al., 2001) by sequestering transducin Gβγ ($G\beta_1\gamma_1$) from the rod outer segment plasma membrane after rhodopsin activation. PDC binds with high affinity to $G\beta_1\gamma_1$ as well

This research was supported by the Intramural Research Program of the National Institutes of Health, National Institute on Alcohol Abuse and Alcoholism.

[1] Current affiliation: Department of Physiology and Biophysics, Georgetown University, Washington, DC.

Article, publication date, and citation information can be found at http://molpharm.aspetjournals.org.
doi:10.1124/mol.105.021394.

ABBREVIATIONS: GPCR, G-protein-coupled receptor; GRK, G-protein-coupled receptor kinase; ctGRK2, carboxyl terminus of GRK2; PDC, phosducin; PDCL, phosducin-like protein; FRET, fluorescence resonance energy transfer; SCG, superior cervical ganglia; ORF, open reading frame; EGFP, enhanced green fluorescent protein; GppNHp, guanylyl imidophosphate; PBS, phosphate-buffered saline; ANOVA, analysis of variance; HEK, human embryonic kidney; $mGlu_2$, metabotropic glutamate receptor type 2.

as to several other Gβγ combinations (Lee et al., 1987; Müller et al., 1996). The crystal structure of the PDC/$G\beta_1\gamma_1$ complex reveals that the N terminus of PDC contains three α-helices whereas the C-terminal portion comprises β-sheets with overall homology to bacterial thioredoxin (Gaudet et al., 1996, 1999; Loew et al., 1998). The N-terminal domain of PDC contacts regions of Gβ common to the interface between Gα and Gβγ in the heterotrimer. Thus, binding of PDC to Gβγ occludes re-association of Gβγ with the Gα subunit (Xu et al., 1995). Structural analyses also indicate that PDC induces a conformational change in Gβγ that buries the isoprenyl group of Gγ within the seven-bladed β-propeller structure of Gβ, thereby decreasing the affinity of Gβγ for the lipid bilayer (Lukov et al., 2004).

A homolog of PDC, phosducin-like protein (PDCL), was discovered during a screen for ethanol-responsive genes (Miles et al., 1993). Although less is known about its cellular functions, PDCL exhibits a more ubiquitous expression pattern (Schröder and Lohse, 2000), binds Gβγ with high affinity, and potentially regulates G-protein receptor function (Schröder and Lohse, 1996; Shulz et al., 1998). The N-terminal domain of PDCL is alternatively spliced and larger than the N-terminal domain of PDC. At present, high-resolution structures of PDCL in complex with Gβγ are unavailable although biochemical studies indicate that heterologously expressed PDCL acts similarly to PDC by binding to and solubilizing Gβγ (Thibault et al., 1997; Lukov et al., 2004). Recent studies, however, indicate that natively expressed PDCL may act as a chaperone within the biosynthetic pathway of Gβ and facilitate assembly with Gγ (Humrich et al., 2005; Knol et al., 2005; Lukov et al., 2005).

G-protein-coupled receptors are popular targets for pharmacological agents. The above structural characteristics of PDC and PDCL provide a rational basis for their use as biosensors of G-protein activation and could facilitate the discovery of new GPCR-targeted drugs via high-throughput assays. Techniques such as fluorescence resonance energy transfer (FRET) (Miyawaki, 2003) and protein complementation (Hu and Kerpolla, 2003) are amenable to high-throughput detection and rely on the dynamic interaction of distinct sensor components. An assay based on these techniques could benefit from the bipartite structure of these Gβγ binding proteins. For example, knowledge of the crystal structure of the PDC-Gβγ complex makes conformational optimization via techniques such as circular permutation possible. In addition, changes in binding affinity with phosphorylation (Gaudet et al., 1999; Thulin et al., 2001; Humrich et al., 2003), and promiscuity in Gβγ binding (Müller et al., 1996) may provide a means of producing a tunable and universal detector of free Gβγ after receptor stimulation.

In this report, we show that heterologous expression of PDC or PDCL in rat superior cervical ganglia (SCG) neurons attenuated GPCR-mediated voltage-dependent inhibition of N-type Ca^{2+} channels ($Ca_V2.2$). Unlike other Gβγ scavengers, PDC and PDCL require prolonged application of agonist before signification effects on modulation were realized. Western blot analysis demonstrated the presence of PDCL, but not PDC, in SCG neurons, suggesting a possible role for this protein in neurotransmitter signaling. We also discuss the possible use of these Gβγ binding proteins as biosensors for G-protein activation.

Materials and Methods

Vectors and DNA Constructs. The open reading frame (ORF) of human PDC (GenBank accession number NM_002597) and rat PDCL (accession number NM_022247) were amplified by reverse transcription-polymerase chain reaction from retinal and dorsal root ganglion mRNA, respectively. The PDC and PDCL ORFs were subcloned into the mammalian expression vector pCI (Promega Corp, Madison, WI) at the XbaI/SmaI sites and EcoRI/NotI sites, respectively. Fusion protein constructs were made by ligating PDC and PDCL ORFs into the multiple cloning sites of various pEGFP vectors (Clontech, Mountain View, CA). All clones were sequenced to verify the fidelity of the cloning process with a DNA sequencer (Beckman Coulter, Fullerton, CA).

Isolation and Injection of Rat SCG Neurons. Adult male rats were used as a source for sympathetic neurons. After dissection of the SCG, ganglia were de-sheathed, minced, and exposed to Earle's balanced salt solution containing 0.06 mg/ml collagenase D (Roche Diagnostics, Indianapolis, IN), 0.03 mg/ml trypsin (Worthington Biochemical Corp, Freehold, NJ), and 0.005 mg/ml DNase I (Sigma-Aldrich, St. Louis, MO). The minced ganglia were then incubated in a shaking water bath for 1 h at 37°C. After incubation, the neurons were dissociated by mechanical disruption, isolated by centrifugation, re-suspended in Eagle's minimal essential medium containing 10% fetal bovine serum and 1% penicillin/streptomycin solution, and plated on 35-mm polystyrene tissue culture dishes coated with poly-L-lysine. After a static incubation of 3.5 to 6 h at 37°C, plasmid DNA was introduced into single neurons via intranuclear injection (Ikeda, 2004) using an Femtojet injection system (Eppendorf, Hamburg, Germany). Plasmid DNA, dissolved in 10 mM Tris/1 mM EDTA, pH 8.0, was injected at concentrations ranging from 5 to 100 ng/μl. A computer-driven, stepper motor-based micromanipulator (Eppendorf 5171) was used to inject neuronal nuclei. Injection pressure was 125 to 200 hPa (1.8–3 psi) for 0.3 s. To visualize successfully injected neurons, 5 ng/μl of pEGFP-N1 was coinjected with the plasmid DNA under study. EGFP fluorescence was visualized 12 to 24 h after injection with a filter cube consisting of an HQ480/40 excitation filter, Q505LP beam splitter, and HQ535/50m emission filter (Chroma Technology Corp, Rockingham, VT), and 100-W mercury arc lamp excitation source. Nonfluorescent neurons served as control cells.

Patch-Clamp Electrophysiology. Whole-cell currents were measured at room temperature (19–21°C) with an Axopatch 200A patch-clamp amplifier (Molecular Devices, Sunnyvale, CA). Recording pipettes were prepared from 7052 borosilicate glass (Garner Glass, Claremont, CA) with a Flaming-Brown puller (Sutter Instrument Co., Novato, CA) and had resistances of 1.5 to 3.0 MΩ when filled with pipette (internal) solution. Pipettes were coated with Sylgard near the tip to reduce capacitance coupling with the bathing solution. The internal solution used to record voltage-gated Ca^{2+} currents contained 120 mM *N*-methyl-D-glucamine, 20 mM tetraethylammonium chloride, 11 mM EGTA, 10 mM sucrose, 0.3 mM Na_2GTP, 1 mM $CaCl_2$, 4 mM MgATP, and 14 mM creatine phosphate. The solution was adjusted to pH 7.2 with methanesulfonic acid, which served as the primary anion, and had an osmolality of ~305 mosmol/kg. The extracellular (bathing) solution contained 140 mM tetraethylammonium-OH, 10 mM $CaCl_2$, 10 mM HEPES, and 15 mM glucose. The solution was adjusted to pH 7.4 with methanesulfonic acid and had an osmolality of 325 to 330 mosmol/kg. The bathing solution was supplemented with 100 nM tetrodotoxin to block endogenous voltage-gated Na^+ channels. Series resistance before electronic compensation (typically 80%) ranged from 2 to 6 MΩ. During recordings, neurons were continuously superfused with external solution. G-protein-coupled receptors were activated by releasing external solution containing agonist over the cell surface using a gravity-driven perfusion system positioned approximately 50 μm from the soma. Drug delivery was controlled electronically via solenoid valves driven by software commands. Currents were low-

pass-filtered at 5 kHz, digitized at a frequency of 10 kHz, and stored on a Macintosh G4 computer using custom developed software. Data were analyzed using the Igor Pro software package (Wavemetrics, Lake Oswego, OR). L-Glutamic acid, (±)-norepinephrine HCl, and guanylyl imidophosphate (GppNHp) were purchased from Sigma-Aldrich. GppNHp was prepared daily at 100× final concentration. Stock solutions of receptor agonists were prepared at 1000× final concentration and stored at −20°C.

Immunoblotting. HEK293 cells were grown to 75 to 90% confluence and transfected with Lipofectamine 2000 (Invitrogen, Carlsbad, CA) according to the manufacturer's instructions. Crude total protein from SCG neurons or transfected HEK293 cells was prepared by re-suspending cells in a lysis buffer containing 10 mM Tris, pH 6.8, supplemented with 0.1% Triton X-100, 1 mM NaF, 1 mM phenylmethylsulfonyl fluoride, and protease inhibitor cocktail (P8340; Sigma-Aldrich). The cell suspension was sonicated six times, and protein concentration was determined with a bicinchoninic acid reagent kit (Pierce Biotechnology Inc., Rockford, IL). Solubilized protein (20 μg/lane) was separated on SDS-polyacrylamide gels according to the method of Laemmli (1970). Separated proteins were electrophoretically transferred (90 min at 25 V) to a polyvinylidene difluoride membrane (Hybond-P; GE Healthcare, Little Chalfont, Buckinghamshire, UK) in blotting buffer consisting of 25 mM Tris base, 191 mM glycine, and 20% (v/v) methanol using an Xcell II blot module (Invitrogen). The membrane was then blocked overnight at 4°C with a solution of 10% (w/v) nonfat dry milk in PBS (consisting of 136 mM NaCl, 10 mM KCl, 32 mM Na_2HPO_4, and 5 mM KH_2PO_4, pH 7.2) then washed three times (10 min/wash) with PBS containing 0.05% (v/v) Tween 20. Rabbit anti-PDC (7.5 μg/ml) or anti-(GST)-PDCL (10 μg/ml) polyclonal antibodies diluted in PBS containing 0.5% (v/v) goat serum, were used to probe the blot for 60 min at room temperature. The primary antibodies were generously provided by Dr. Barry Willardson (Brigham Young University, Provo, UT) and characterized by Thulin et al., (1999). After washing, the blot was incubated with a horseradish peroxidase-labeled goat anti-rabbit IgG (0.5 μg/ml) diluted in PBS containing 0.5% (v/v) goat serum (Upstate, Lake Placid, NY). Antigen was visualized using 3,3′,5,5′-tetramethylbenzidene-stabilized substrate for horseradish peroxidase (Promega Corp., Madison, WI).

Microscopy. Laser scanning, two-photon imaging was performed using a Zeiss 510 META/NLO attached to an upright Zeiss Axioplan 2 microscope with a 20×, 0.5 numerical aperture water-immersion objective (Carl Zeiss AG, Jena, Germany). Fluorescent neurons were excited in two-photon mode with a Chameleon Ti:Sapphire laser (Coherent Inc., Santa Clara, CA) mode-locked at 850 nm. Emitted photons were filtered with at 500 to 550 nm with a bandpass filter and detected on a micro-channel plate photomultiplier (R3809U-52; Hamamatsu Corporation, Bridgewater, NJ). The *z*-axis optical section depth was estimated to be 3.3 μm.

Results

Phosducin Expression Did Not Alter Maximal Ca^{2+} Current Inhibition in SCG Neurons. SCG neurons express α_2-adrenergic receptors (Schofield, 1991) that couple to pertussis toxin-sensitive G-proteins and inhibit N-type voltage-gated Ca^{2+} channels. The inhibition is voltage-dependent and mediated by Gβγ "released" from the activated G-protein heterotrimer. We used this well characterized pathway to examine the impact of PDC or PDCL expression on neurotransmitter-mediated modulation of N-type Ca^{2+} channels.

Plasmid cDNAs encoding PDC and enhanced green fluorescent protein (EGFP) were injected into the nuclei of isolated rat SCG neurons. Uninjected neurons or neurons injected with EGFP cDNA alone served as control cells. It should be noted that some neurons considered "uninjected" may represent unsuccessful injections (i.e., neurons in which insufficient cDNA reached the nucleus to produce detectable fluorescence). Whole-cell, voltage-clamp recordings were performed after overnight incubation at 37°C to allow for protein expression. Ca^{2+} channel current (hereafter, I_{Ca}) was evoked every 10 s with the voltage protocol illustrated in Fig. 1A (top). The protocol, evoked from a holding potential of −80 mV, consisted of a 25-ms test pulse (denoted prepulse) to +10 mV, a 40-ms conditioning depolarizing step to +80 mV, a 10-ms return to −80 mV, and a second 25-ms test pulse (denoted postpulse) to +10 mV (Elmslie et al., 1990). Representative I_{Ca} traces recorded in the absence (con) or presence of norepinephrine are illustrated in Fig. 1A. In control neurons, the mean amplitudes of the prepulse and postpulse currents, measured isochronally 10 ms after the start of the test pulse, were −1.62 ± 0.14 and −2.07 ± 0.17 nA (n = 41), respectively. The ratio of the postpulse-to-prepulse current amplitude in the absence of agonist (termed the basal facilitation ratio) averaged 1.30 ± 0.02 and 1.33 ± 0.04 in uninjected and EGFP-N1-expressing neurons (n = 10; summarized in Fig. 1D). The enhancement of postpulse current amplitude (i.e., facilitation ratio >1) in the absence of agonist has been shown to arise from tonic Gβγ modulation of N-type Ca^{2+} channels in SCG neurons (Ikeda, 1991; Garcia et al., 1998).

Application of norepinephrine (10 μM) to uninjected neurons decreased the prepulse I_{Ca} by 63.4 ± 1.6% (n = 41) and slowed the activation phase of the current (Fig. 1, A and E). Conversely, the postpulse I_{Ca} was inhibited by only 26.2 ± 1.1% and the activation phase remained rapid (Fig. 1A). Similar results were obtained from neurons expressing EGFP alone [prepulse and postpulse I_{Ca} inhibitions of 62.8 ± 3.1 and 24.3 ± 3.4% (n = 10), respectively]. To determine the effects of expressing PDC on N-type Ca^{2+} channel modulation, a cDNA construct consisting of the PDC ORF was cloned into the mammalian expression vector pCI. PDC cDNA was injected into the nuclei of SCG neurons at concentrations ranging from 10 to 100 ng/μl. In 23 neurons coinjected with EGFP and PDC cDNA, application of 10 μM norepinephrine decreased the pre- and postpulse I_{Ca} by 56.8 ± 3.3 and 24.1 ± 2.1%, respectively—values similar to control (Fig. 1E). To ensure that PDC expression was occurring, the ORF of PDC was fused in-frame with EGFP and constructs were injected as above. Fusion of EGFP to either termini of PDC results in small but significant decrease in channel modulation. Application of 10 μM norepinephrine to EGFP-PDC or PDC-EGFP expressing neurons (10–100 ng/μl) resulted in 54.2 ± 3.5 and 54.3 ± 2.8% inhibition of prepulse I_{Ca}, respectively (Fig. 1, C and E).

Expression of Gβγ binding proteins has been shown to reduce the N-type Ca^{2+} current facilitation ratio in the absence of agonist. For example, expression of Gα subunits (Ikeda, 1996; Jeong and Ikeda, 1999) or a myristoylated C-terminal constructs of G-protein coupled receptor kinase 2 (MAS-GRK2; Kammermeier and Ikeda, 1999) reduce the basal facilitation ratio. In neurons injected with 10 to 100 ng/μl of PDC cDNA, the mean basal facilitation ratio was 1.19 ± 0.03—a value significantly different from control neurons (Fig. 1D, one-way ANOVA, Dunnett's test). Likewise, expression of the EGFP fusion constructs reduced the basal facilitation ratio (summarized in Fig. 1D).

In contrast, manipulations that increase free G$\beta\gamma$ result in a greater facilitation ratio. For example, activation of adrenergic receptors by agonists increases the ratio of postconditioning-to-preconditioning pulse current amplitude. This maximal or agonist–induced facilitation ratio determined in the presence of 10 μM norepinephrine was decreased by PDC expression (summarized in Fig. 1F). The peak facilitation ratio increased to 2.74 ± 0.09 and 2.78 ± 0.12 in uninjected and EGFP-expressing cells, respectively, in the presence of agonist. These values averaged 2.32 ± 0.12, 2.22 ± 0.16, and 2.18 ± 0.11 in the PDC, EGFP-PDC, and PDC-EGFP injection conditions, respectively. The relief of block after a strong depolarization (resulting in an increased facilitation ratio) and the slowed current activation time course are characteristic features of G$\beta\gamma$-mediated voltage-dependent inhibition of Ca^{2+} channels (reviewed by Jarvis and Zamponi, 2001).

Phosducin Expression Produced a Time-Dependent Decrease in Voltage-Dependent Ca^{2+} Channel Modulation. Although PDC expression produced only modest effects on the maximal voltage-dependent inhibition of N-type Ca^{2+} channels by norepinephrine, more substantial effects were observed during prolonged agonist application. In control SCG neurons, a 5-min continuous exposure to agonist (Fig. 2A) produced a sustained I_{Ca} inhibition that decreased gradually during the agonist application. The norepinephrine-mediated inhibition of the prepulse I_{Ca} decreased to 41.9 ± 2.1 and 39.9 ± 4.5% of initial values after 5 min of agonist exposure in uninjected (n = 41) and EGFP-expressing (n = 10) neurons, respectively (Fig. 2A). Expression of PDC, EGFP-PDC, or PDC-EGFP accelerated the rundown of prepulse I_{Ca} inhibition (example shown for PDC-EGFP in Fig. 2B). At the fifth minute of drug application, the inhibition of I_{Ca} averaged 28.4 ± 3.4, 17.7 ± 3.1, and 23.2 ± 2.5% in neurons injected with PDC (n = 22), EGFP-PDC (n = 20), and PDC-EGFP (n = 25), respectively (summarized in Fig. 2C). In control neurons, the mean agonist facilitation ratio at the end of norepinephrine exposure was 1.99 ± 0.06 and 1.98 ± 0.08 in EGFP-injected cells. The agonist facilitation ratio after 5-min agonist exposure averaged 1.52 ± 0.07, 1.34 ± 0.06, and 1.40 ± 0.04 in PDC (n = 22), EGFP-PDC (n = 20), and PDC-EGFP (n = 25) expressing neurons (summarized in Fig. 2D). The decrease in agonist facilitation ratio during agonist application indicates a fading of the G$\beta\gamma$-mediated I_{Ca} inhibition process in PDC-expressing neurons. Consistent with this, the prepulse current activated more rapidly in neurons expressing PDC at the end of the agonist application (data not shown).

Expression of Phosducin Suppressed Ca^{2+} Channel Recovery from Inhibition after Agonist Treatment. It has been hypothesized that phosducin decreases the affinity of free G$\beta\gamma$ subunits with the plasma membrane, thereby causing the heterodimer to dissociate from the plasma membrane (Lukov et al., 2004). If these events occur, then voltage-dependent inhibition of Ca^{2+} channels would be expected to diminish upon reapplication of agonist. To probe this question, SCG neurons were exposed to norepinephrine for 5 min, washed with agonist-free solution for 3 min, and then rechallenged with norepinephrine (Fig. 2E). During the second

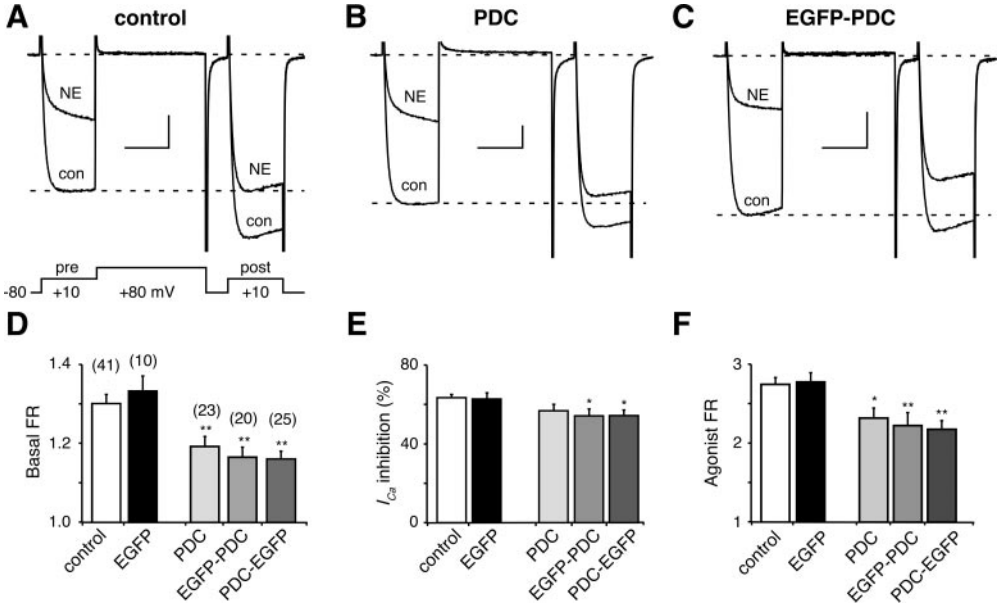

Fig. 1. Effect of phosducin expression on N-type Ca^{2+} channel modulation in sympathetic neurons. A, superimposed Ca^{2+} current (I_{Ca}) traces from an uninjected control neuron recorded using the whole-cell patch-clamp technique. I_{Ca} was elicited from a holding potential of −80 mV using the voltage protocol illustrated (bottom) in the absence (con) or presence of 10 μM norepinephrine (NE). I_{Ca} elicited by the first test pulse to +10 mV are denoted prepulse currents (pre). After the depolarizing conditioning pulse to +80 mV, I_{Ca} elicited by the subsequent test pulse are denoted postpulse currents (post). Facilitation ratio (FR), a measure of G$\beta\gamma$-mediated I_{Ca} modulation, was determined as the post/pre I_{Ca} amplitude ratio (see lower dashed line). Capacitance transient and peak tail currents have been truncated. The zero current level in this and subsequent figures is denoted by a dashed line. Vertical and horizontal calibration were 0.5 nA and 20 ms, respectively. B, superimposed sample currents from neurons expressing phosducin (PDC) in absence (con) or presence (NE) of 10 μM norepinephrine. C, representative I_{Ca} traces from neurons expressing EGFP-PDC in the absence (con) or presence (NE) of 10 μM norepinephrine. D, bar graph summary of the mean (+S.E.M.) facilitation ratio in the absence of agonist (termed basal FR). E, summary bar graph of mean (+S.E.M.) prepulse I_{Ca} inhibition evoked by norepinephrine. F, bar graph summary of the mean (+S.E.M.) peak facilitation ratio determined in the presence of norepinephrine (termed agonist FR). The open and filled bars represent basal facilitation ratio from uninjected and EGFP-expressing neurons. The filled gray bars represent basal facilitation ratio from neurons expressing the indicated PDC constructs. Asterisks above bars in this and subsequent figures indicates significance of $p < 0.05$ (*) or $p < 0.01$ (**) compared with control responses as determined using one-way ANOVA and Dunnett's post hoc test. Numbers in parentheses denote the number of neurons tested.

agonist application, the mean peak inhibition was 55.6 ± 1.9% in control cells (n = 21), 58.8 ± 4.0% in EGFP-injected cells (n = 8), 29.1 ± 4.2% in PDC-injected cells (n = 17), 34.4 ± 3.8% in EGFP-PDC injected cells (n = 13), and 35.0 ± 2.9% in PDC-EGFP injected cells (n = 18). In all PDC expression conditions, a statistically significant difference was observed compared with control measurements (ANOVA, $p < 0.01$, Dunnett's test). Although control neurons nearly returned to peak inhibition conditions, neurons expressing PDC displayed partial recovery of inhibition after agonist washout (Fig. 2F).

Phosducin-Like Protein Affects N-Type Ca^{2+} Channel Modulation Mediated by α_2-Adrenoceptors. PDCL is ~65% homologous with PDC and binds the G$\beta\gamma$ heterodimer in vitro (Schroder et al., 1996). However, unlike PDC, PDCL has a more widespread expression pattern, making it a candidate for modulating GPCR signaling in neurons. At present, it is unclear whether PDCL affects GPCR-mediated inhibition of I_{Ca}. Therefore, SCG neurons were injected with PDCL cDNA, and N-type Ca^{2+} channel modulation was tested. After expression of PDCL, peak I_{Ca} inhibition was unaffected. In neurons injected with 10 to 50 ng/μl pCI-PDCL cDNA, the mean prepulse inhibition was 51.7 ± 3.1% (n = 16; Fig. 3B) versus 55.1 ± 2.5% (n = 32) for control neurons (Fig. 3, A and D). The mean peak facilitation ratio during agonist application was also not altered by PDCL expression (2.28 ± 0.10 versus 2.00 ± 0.13 for control and PDCL-expressing neurons, respectively; $p > 0.05$, ANOVA). In contrast, the mean basal facilitation ratio was decreased by PDCL expression (Fig. 3C). In control neurons, the mean basal facilitation ratio was 1.21 ± 0.02, whereas in PDCL-injected neurons, it decreased to 1.12 ± 0.02 ($p < 0.05$, ANOVA). As with expression of PDC, PDCL caused a more rapid disinhibition of I_{Ca} in the continued presence of agonist (Fig. 3B). After 5 min of exposure to 10 μM norepinephrine, the peak prepulse inhibition averaged 31.5 ± 2.2% (n = 24) in control cells, whereas in neurons expressing PDCL, peak inhibition averaged 22.1 ± 2.7% (n = 13; Fig. 3E). The corresponding mean facilitation ratio at the end of the drug application averaged 1.56 ± 0.04 in control cells and 1.25 ± 0.04 in PDCL-injected cells. As with PDC, expression of PDCL maintained suppression of inhibition upon rechallenging neurons with 10 μM norepinephrine. During the rechallenging period, 17 control neurons were inhibited by 41.0 ± 3.1%, whereas in nine

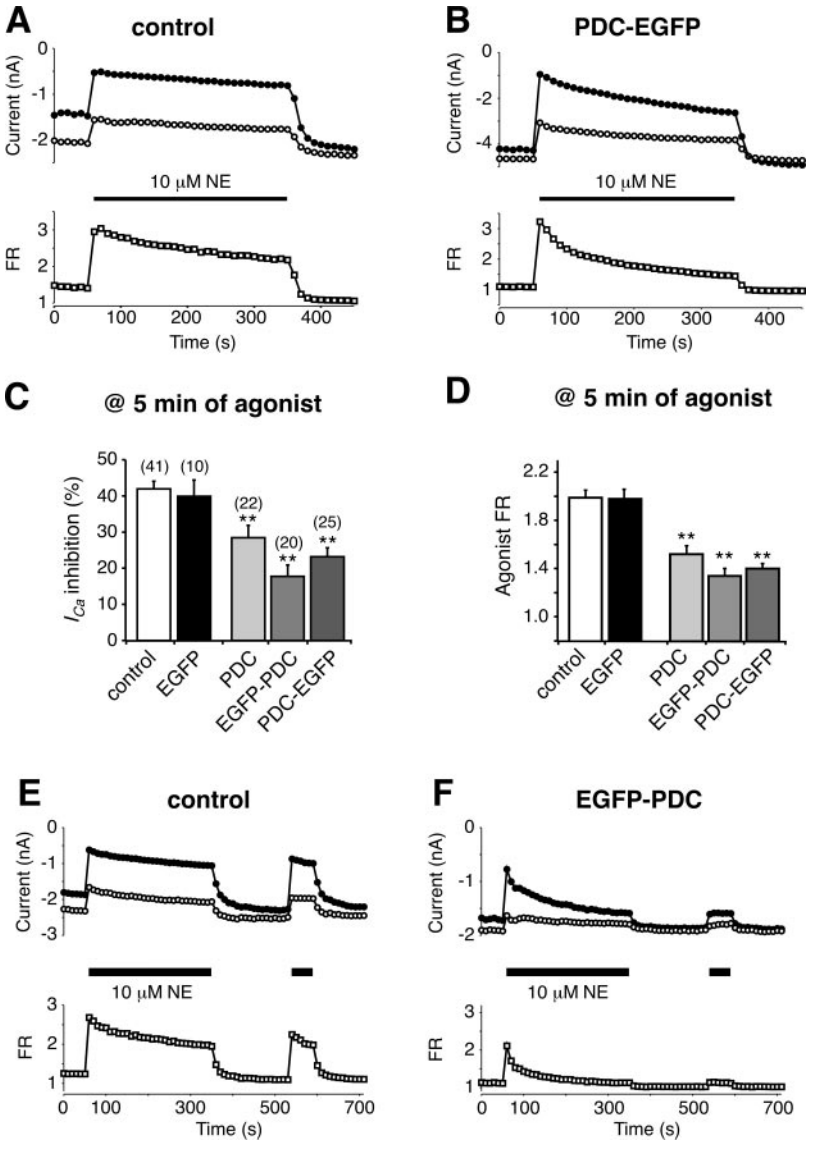

Fig. 2. Effects of phosducin during prolonged agonist application. A and B, time courses of I_{Ca} amplitude during a five min agonist exposure. Top, ● and ○ represent the prepulse and postpulse I_{Ca} amplitudes, respectively. The solid bar indicates the duration of norepinephrine exposure. Bottom, the facilitation ratio (□) plotted as a function of time. Neurons were either uninjected (A) or injected with PDC-EGFP cDNA (B). Note the more rapid decay of I_{Ca} inhibition and facilitation ratio in B. C, summary bar graph of mean (+S.E.M.) I_{Ca} inhibition after 5 min of continuous norepinephrine (10 μM) application. D, bar graph summary of mean facilitation ratio (+S.E.M.) after 5 min of norepinephrine exposure. The open and filled bars represent basal facilitation ratio from uninjected and EGFP-expressing neurons. E and F, time courses of I_{Ca} amplitudes during a 5-min and rechallenge agonist exposure. Top, prepulse (●) and postpulse (○) I_{Ca} amplitudes from an uninjected neuron (E) and a neuron expressing EGFP-PDC (F). Solid bars represent the two periods of norepinephrine (10 μM) application. Bottom, time course of facilitation ratio change.

neurons expressing PDCL, I_{Ca} was inhibited by 25.8 ± 4.7%. PDCL fusion proteins at the amino and carboxyl termini with EGFP were also made and injected into SCG neurons. In six neurons injected with PDCL-EGFP, peak I_{Ca} inhibition by 10 μM norepinephrine averaged 62.5 ± 4.8%. In four neurons injected with the EGFP-PDCL, this value averaged 59.8 ± 6.1%.

Phosducin-like Protein, but Not Phosducin, Is Endogenously Expressed in SCG Neurons. To determine whether PDC or PDCL was endogenously expressed in SCG neurons, Western blot analyses were performed. The affinity-purified polyclonal antibodies against PDC (anti-PDC) and the N terminus of PDCL (anti-PDCL) were a gift from Dr. Barry M. Willardson (Brigham Young University, Provo, UT) and have been characterized previously (Thulin et al., 1999). In HEK-293 cells transfected with PDC cDNA, the anti-PDC antibody recognized a protein with an apparent molecular mass of ~31 kDa (Fig. 4A, lane 3), consistent with the expected size of the PDC protein (Thulin et al., 1999). An immunoreactive band corresponding to PDC was not detected in protein prepared from SCG neurons or HEK-293 cells mock-transfected with an empty expression vector (Fig. 4A, lanes 1 and 2). As a test for antibody specificity, HEK-293 cells were transfected with a plasmid encoding PDCL. The anti-PDC antibody weakly detected a protein with an apparent molecular mass of ~42 kDa, probably corresponding to overexpression of PDCL (Fig. 4A, lane 4). This weak cross-reactivity of anti-PDC for PDCL is in agreement with the previous characterization of the antibody (Thulin et al., 1999). Similar experiments performed on protein prepared from SCG neurons using an anti-PDCL antibody revealed two immunoreactive bands with apparent molecular masses of ~42 and ~40 kDa (Fig. 4B, lane 1). The positions of these two immunoreactive proteins are consistent with the expected sizes of the PDCL protein as seen by, and discussed in, Thulin et al. (1999). Immunoreactivity of comparable size was detected in HEK cells transfected with an empty expression vector or expression vectors containing PDC or PDCL (Fig. 4B, lanes 2–4). In contrast to the anti-PDC experiment, and, despite weak immunoreactivity of the anti-PDCL for PDC during characterization of the antibody by Thulin et al. (1999), a 31-kDa PDC band was not observed in our system upon overexpression of PDC in HEK-293 cells. However, the specificity of the anti-PDCL is supported by the observation that in Fig. 4B, lane 4, the HEK-293 cells overexpressing the PDCL protein clearly display a larger amount of antigen detected under identical conditions as HEK cell untransfected or transfected with PDC. If the antibodies were not specific for PDCL, the same level of immunoreactive product would be present in all lanes loaded with protein from HEK-293 cells. Overall, these results suggest that PDCL is endogenously expressed in HEK-293 cells and SCG neurons.

The subcellular distribution of heterologously expressed PDC and PDCL were examined using confocal microscopy.

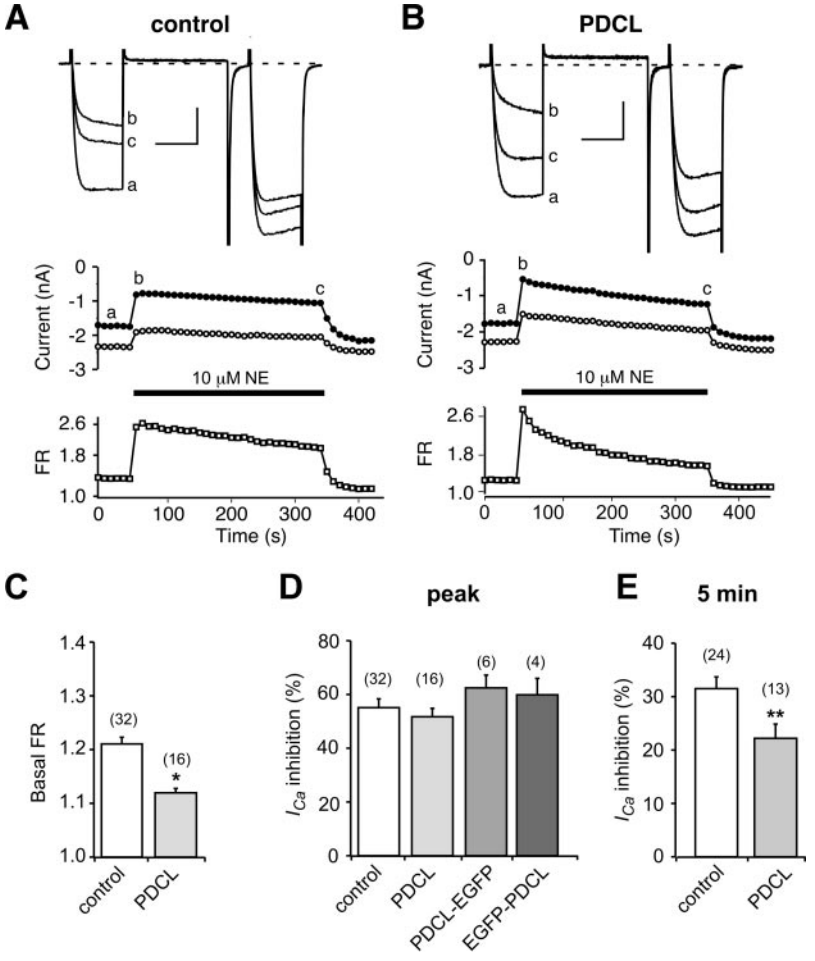

Fig. 3. Effects of PDCL expression on N-type Ca^{2+} channel modulation. A and B, top, superimposed I_{Ca} traces corresponding to time points denoted by lowercase letters (a–c, middle). Vertical and horizontal calibration are 0.5 nA and 20 ms, respectively. Middle, time course of prepulse (●) and postpulse (○) I_{Ca} amplitude during prolonged norepinephrine (10 μM) application (solid bar) to a control (A) or PDCL-expressing (B) neuron. Lowercase letters above plot correspond in time to I_{Ca} traces shown to the top. Bottom, the facilitation ratio (□) plotted as a function of time. Neurons were either uninjected (A) or injected with PDCL cDNA (B). C–E, bar graph summaries of mean (+S.E.M.) basal facilitation ratio (C), I_{Ca} inhibition at the start of (D), or after 5-min exposure to norepinephrine (E). Statistically significant difference in (C and E) was determined using unpaired Student's *t* test.

Injection of either the amino-terminal (EGFP-PDC) or the carboxyl-terminal (PDC-EGFP) fusion constructs (10–100 ng/ml) resulted in green fluorescence throughout the cytoplasm and nucleus of SCG neurons (Fig. 4C). Upon expression of PDCL-EGFP protein, green fluorescence was observed within the cytoplasm but restricted from the nucleus in both SCG neurons (Fig. 4D) and HEK-293 cells (data not shown).

Phosducin and Phosducin-Like Protein Expression Disinhibited Voltage-Dependent I_{ca} Mediated by $mGlu_2$ Activation. To test the generality of PDC and PDCL effects on Ca^{2+} channel modulation, we examined voltage-dependent inhibition mediated by metabotropic glutamate receptor type 2 ($mGlu_2$), a type III GPCR. The $mGlu_2$ receptor couples to $G\alpha_{i/o}$ family of proteins and has been shown to inhibit N-type Ca^{2+} channels in a voltage-dependent fashion that involves $G\beta\gamma$ in SCG neurons (Kammermeier et al., 2003). Heterologous expression of $mGlu_2$ in SCG neurons produces a robust inhibition upon glutamate application that is consistent and rapidly reversible.

The amplitude of I_{Ca} recorded from uninjected neurons were minimally affected by application of 100 μM L-glutamate (2.9 $\pm$ 1.1% inhibition, $n = 11$) supporting previous studies showing that SCG neurons do not express functional mGlu receptors. Before agonist application, the basal facilitation ratio averaged 1.14 $\pm$ 0.02, 1.03 $\pm$ 0.02, and 1.12 $\pm$ 0.03 in $mGlu_2$ ($n = 14$), $mGlu_2$/PDC ($n = 10$), and $mGlu_2$/PDCL ($n = 13$) conditions, respectively ($mGlu_2$/PDC statistically different at $p < 0.01$ from both $mGlu_2$ and $mGlu_2$/PDCL; ANOVA with Dunnett's post hoc test). After application of 100 μM L-glutamate to neurons previously injected with pCI-$mGlu_2$ cDNA (50 ng/μl), prepulse I_{Ca} was inhibited by 64.5 $\pm$ 2.8% ($n = 14$; Fig. 5A). In the continued presence of L-glutamate for 5 min, I_{Ca} inhibition decreased to 41.2 $\pm$ 1.9%, a result similar to that seen with endogenous α_2-adrenoceptor activation. PDC or PDCL cDNA (25–50 ng/μl) was coinjected with the $mGlu_2$ cDNA and EGFP. When $mGlu_2$ and PDC were coexpressed, the mean peak prepulse inhibition was 61.1 $\pm$ 2.5% ($n = 10$) and decreased to 22.7 $\pm$ 3.6% in the continued presence of L-glutamate for 5 min (Fig. 5, D and E). When $mGlu_2$ and PDCL were coexpressed, peak I_{Ca} inhibition averaged 51.4 $\pm$ 3.1% ($n = 13$) and decreased to 17.0 $\pm$ 3.1% by the fifth minute of agonist exposure (Fig. 5, D and E). The decrease in the peak inhibition was significantly different when comparing neurons expressing $mGlu_2$ alone and those expressing PDCL (ANOVA, Dunnett's test, $p < 0.05$; Fig. 5D). The corresponding facilitation ratios at the end of the L-glutamate application averaged 1.62 $\pm$ 0.04, 1.20 $\pm$ 0.05, and 1.24 $\pm$ 0.04 in the $mGlu_2$, $mGlu_2$/PDC, and $mGlu_2$/PDCL conditions, respectively (ANOVA, Dunnett's test, $p < 0.001$ for both experimental conditions).

Phosducin and Phosducin-like Protein Delay Voltage-Dependent Inhibition Mediated by Direct G-Protein Activation. The accelerated disinhibition kinetics shown above could result from PDC or PDCL acting directly on the receptor (e.g., desensitization or coupling to the G-protein). To examine this possibility, GppNHp, a nonhydrolyzable analog of GTP, was included in the patch pipette solution, thereby bypassing receptor activation as the initiator of modulation. Because GppNHp traps the Gα subunit in an activated state, G$\beta\gamma$ subunits are free to interact with effectors such as Ca^{2+} channels. The normal internal solution containing 300 μM GTP did not alter the pre- or post-

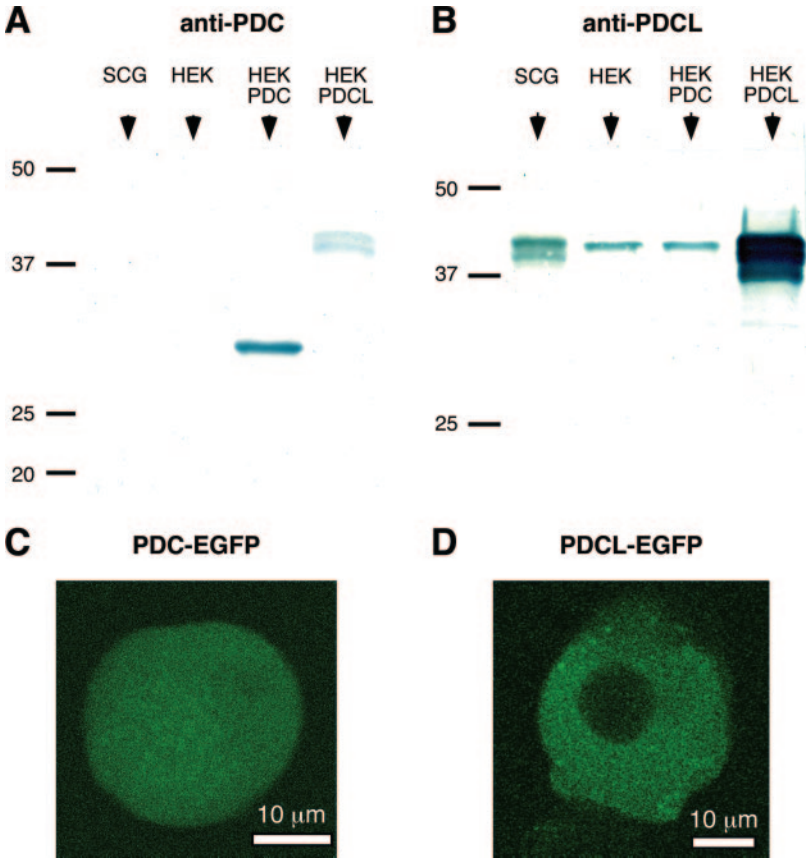

Fig. 4. Native expression and subcellular localization of PDC and PDCL in sympathetic neurons. A and B, Western blot of Triton X-100 soluble crude protein prepared from SCG neurons and HEK-293 cells probed with a rabbit anti-PDC (A) or rabbit anti-PDCL (B) antibody. An equivalent amount of protein (20 μg) was analyzed from SCG neurons, mock transfected HEK-293 cells, or HEK-293 cells transfected with pCI-PDC or pCI-PDCL cDNA as indicated (left to right). The mobility of molecular mass standard proteins (kilodaltons) is indicated by horizontal bars to the left of each blot. C and D, images of SCG neurons expressing PDC-EGFP (C) or PDCL-EGFP (D). Scale bar corresponds to 10 μm.

conditioned Ca^{2+} current amplitude over 8 to 10 min of recording (data not shown). Conversely, inclusion of GppNHp (500 μM) in the patch pipette resulted in a decrease in I_{Ca} amplitude, slowing of current activation, and increase in facilitation ratio within minutes of patch rupture (Fig. 6). Shown in Fig. 6A are the time courses of facilitation ratio enhancement by GppNHp in control neurons and in those expressing PDC and PDCL. PDC and PDCL expression delays the onset of I_{Ca} inhibition. These data are consistent with PDC and PDCL acting in the absence of receptor activation.

Discussion

Herein, we provide evidence that 1) PDC and PDCL attenuate G$\beta\gamma$-mediated N-type Ca^{2+} channel modulation during prolonged treatment with agonist but have minimal impact on short-term modulation; 2) both natively and heterologously expressed GPCR functions are modified by PDC and PDCL expression; 3) encumbering either the N or C terminus of PDC and PDCL with EGFP does not interfere with function; and 4) PDCL, but not PDC, is expressed in sympathetic ganglia. The motivations underlying the study were to provide 1) information on the suitably of PDC or PDCL as the basis for a universal optical sensor of heterotrimeric G-protein activation by GPCRs, and 2) insight into possible physiological roles for PDC/PDCL modification of GPCR responses in neurons.

A protein-based optical sensor for G-protein activation would facilitate investigation into the temporal and spatial aspects of GPCR function in living cells and provide the basis for high-throughput drug screening. To be widely applicable across a board spectrum of GPCRs, a suitable sensor should detect an event universal to G-protein activation rather than rely on interactions with downstream effectors specific to G-protein families. For example, changes in intracellular $[Ca^{2+}]$ or [cAMP] are associated with the $G_{q/11}$ and G_s/G_i families, respectively, and thus cannot be used as a universal monitor of GPCR activity without heterologously expressing chimeric Gα or providing Gα proteins, such as $G\alpha_{15/16}$, that promiscuously couple to receptors. We thus focused on the

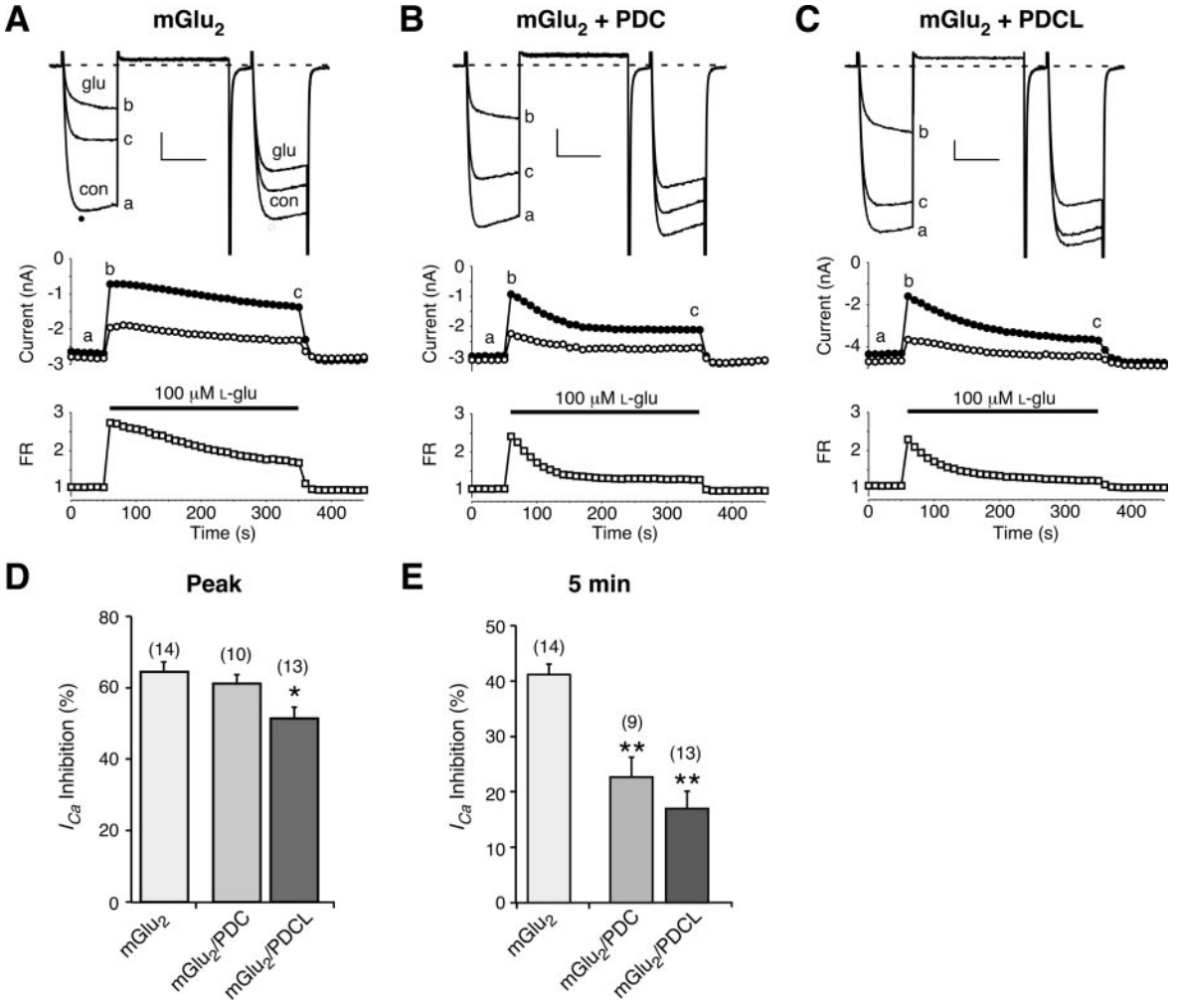

Fig. 5. Phosducin and phosducin-like protein attenuate $mGlu_2$-mediated voltage-dependent inhibition of Ca^{2+} channels. A–C, top, superimposed I_{Ca} recordings from neurons coinjected with EGFP and $mGlu_2$ (A), $mGlu_2$/PDC (B), and $mGlu_2$/PDCL (C), in the absence (con) or presence (glu) of L-glutamate (100 μM). Letters adjacent to traces (a–c) denote time during which traces were sampled as annotated on the plots below. Horizontal and vertical calibration (A–C) are 0.5 nA and 20 ms, respectively. Middle, time courses of I_{Ca} amplitude during a 5-min exposure to L-glutamate (solid bar). The ● and ○ represent the prepulse and postpulse I_{Ca} amplitudes, respectively. Lowercase letters correspond to I_{Ca} traces. Bottom, the facilitation ratio (□) plotted as a function of time. D and E, bar graph summaries of the mean (+ S.E.M.) I_{Ca} inhibition mediated by 100 μM L-glutamate at the peak (D, time "b") and after 5 min of exposure to agonist (E, time "c") for $mGlu_2$ (open), $mGlu_2$/PDC (light gray), or $mGlu_2$/PDCL (dark gray) expressing neurons.

initial event in G-protein activation, dissociation of the Gα from the Gβγ subunit. Although it is unclear whether the classic view of Gα-GTP and Gβγ dissociating into "free" subunits is correct (Bünemann et al., 2003), there is general agreement that activation of heterotrimeric G-proteins involves both conformational changes resulting from GTP binding to Gα and exposure of regions of Gβγ previously masked by tight association with Gα. Thus, a Gβγ-binding protein that bound to regions of Gβγ exposed upon receptor activation could detect activation of a wide variety of GPCRs.

Of the Gβγ-binding proteins for which a high resolution structures are available (PDC, Gα, and GRK2), PDC was attractive for several reasons. First, PDC consists of two independent domains (Savage et al., 2000) that bind to distinct surfaces of Gβ (Gaudet et al., 1996, 1999; Loew et al., 1998). The PDC N terminus interacts with the top of the Gβ propeller sharing many residues normally masked by Gα-GDP in the heterotrimeric state. The C terminus of PDC resembles a thioredoxin domain and interacts with residues on the side of the Gβ propeller distinct from any of those used by Gα-GDP. The two-domain structure would facilitate two common strategies used to develop protein-based optical sensors: FRET (see review by Miyawaki, 2003) and protein complementation (Hu and Kerpolla, 2003). Both strategies rely on bringing separate protein moieties (two different fluorescent proteins or two halves of the same fluorescent protein, respectively) into close proximity upon target binding. Knowledge of the PDC-Gβγ structure provides a rational basis for engineering a sensor using techniques such as circular permutation (Nagai et al., 2001) to optimize the proximity of fluorophores or protein domains upon PDC binding to Gβγ. Second, PDC, although interacting natively only with tranducin $G\beta_1\gamma_1$, binds to numerous different Gβγ combinations in vitro (Müller et al., 1996) suggesting the ability to modify activation by numerous G-protein families. Third, the affinity of PDC and PDCL for Gβγ is altered by phosphorylation of identified residues (Gaudet et al., 1999; Thulin et al., 2001; Humrich et al., 2003) thus providing a rational basis for fine-tuning the interaction.

To evaluate how heterologous expression of PDC and PDCL affected GPCR function in neurons, N-type Ca^{2+} channel function in sympathetic neurons was examined. In this system, voltage-dependent Ca^{2+} channel modulation via Gβγ after GPCR activation has been well characterized (e.g., Ikeda, 1996) and the effects of Gα-GDP and the carboxyl terminus of GRK2 (ctGRK2), two other Gβγ-binding proteins, documented (Jeong and Ikeda, 1999; Kammermeier and Ikeda, 1999). The finding that PDC and PDCL had little effect on basal facilitation (an indicator of tonic Gβγ-mediated Ca^{2+} channel inhibition) or maximal voltage-dependent inhibition of N-type Ca^{2+} channels (Fig. 1) was unexpected because heterologous expression of Gαs and ctGRK2 greatly attenuated peak inhibition. A possible explanation for this difference is that PDC and PDCL are cytosolic proteins, whereas the latter molecules were targeted to the plasma membrane (the ctGRK used previously was targeted to the membrane via an N-terminal myristolyation sequence; Kammermeier and Ikeda, 1999). In support of this idea, Rishal et al. (2005) found that targeting PDC to the membrane (via a myristoylation sequence) increased the ability of PDC to modify basal and GPCR-activated GIRK-type K^+ channels in *Xenopus laevis* oocytes. Preliminary data from our laboratory using analogous constructs resulted in similar augmented effects on Ca^{2+} channels in sympathetic neurons (J. G. Partridge, unpublished observations). Prolonged application of agonist indicate that PDC and PDCL function like other Gβγ buffers but require more time before substantial effects are realized (Figs. 2 and 3). Schulz et al. (1998) describe a mechanism whereby a PDC-EGFP fusion protein concentrates at the plasma membrane within 2 to 3 min of prostaglandin receptor stimulation in NG108 neuroblastoma cells—a result similar to the time course we observed in SCG neurons. The lack of an immediate effect on Ca^{2+} channel modulation provides evidence that heterologously expressed PDC and PDCL were not competing with Gα-GDP for Gβγ and thereby uncoupling GPCRs from G-proteins before receptor stimulation. Such an effect would decrease the signal from an optical sensor as a significant fraction might be bound to Gβγ before receptor stimulation.

Fusing EGFP to either the N or C terminus of PDC/PDCL (Figs. 1–3) had no discernible effect compared with wild-type constructs. Thus, as predicted from high-resolution structures, these regions do not seem to participate in the binding of PDC/PDCL to Gβγ. In addition, the steric bulk introduced by fusing EGFP did not seem to hinder accessibility to binding surfaces of Gβγ exposed after receptor stimulation. Because enhanced cyan fluorescent protein and enhanced yellow fluorescent protein variants represent the current choice

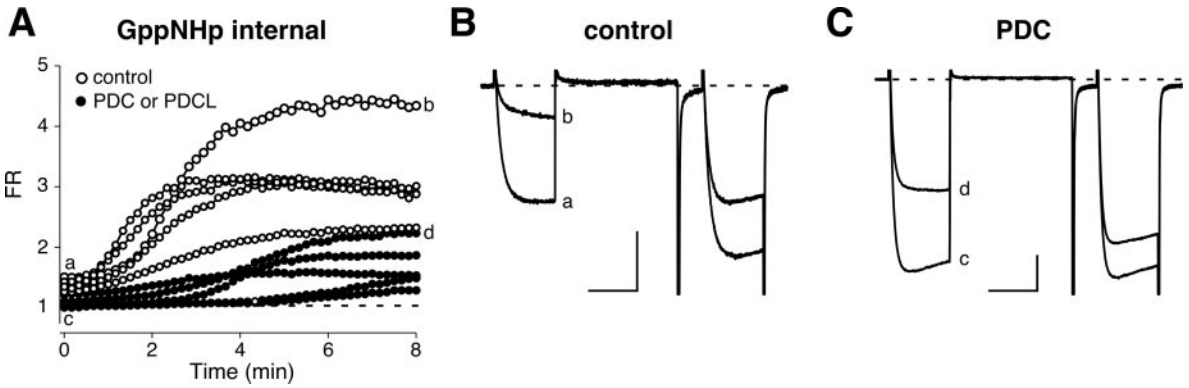

Fig. 6. Phosducin and phosducin-like protein delay the onset of GppNHp-induced Ca^{2+} current facilitation. A, facilitation ratio time courses of five uninjected neurons (○) and five neurons injected with PDC or PDCL cDNA (●) dialyzed with 500 μM GppNHp from the patch pipette. Facilitation ratio was determined at 10-s intervals after rupture of the cell membrane. Lowercase letters (a–d) correlate to I_{Ca} traces obtained at the indicated times for a control neuron (B) and a neuron injected with PDC cDNA (C). Vertical and horizontal calibration are 1 nA and 20 ms, respectively.

for genetically encoded FRET-based sensors, the absence of effects after EGFP fusion suggests a compatibility with this approach. The subcellular fluorescence patterns observed with PDC or PDCL fusion proteins to EGFP (Fig. 4, C and D) were consistent with PDCL, but not PDC, forming a complex with sufficient mass to be excluded from the nucleus. Concerning this observation, PDCL (but not PDC) was recently shown to complex with a chaperone, TCP1α, which regulates the assembly of the G$\beta\gamma$ dimer (Humrich et al., 2005; Lukov et al., 2005). This finding makes PDCL a less desirable candidate for development as an optical sensor.

The generality of PDC and PDCL actions was tested by heterologously expressing a class III GPCR, the $mGlu_2$ receptor. In general, disinhibition of Ca^{2+} channel modulation was similar to that observed with natively expressed class I α_2-adrenoceptors (Fig. 5). This suggests that PDC and PDCL can generally influence GPCR mediated signaling—at least in regard to receptors that preferentially couple to $G_{i/o}$ proteins. It is unclear whether α_2-adrenoceptors and $mGlu_2$ receptors couple to distinct G$\beta\gamma$ isoforms. However, these results are consistent with biochemical studies indicating that PDC can bind numerous G$\beta\gamma$ combinations (Müller et al., 1996). The results of the rechallenging experiments (Fig. 2, E and F) demonstrate that the effects of PDC and PDCL did not readily reverse. This characteristic could decrease the temporal resolution of a sensor but provide some advantage for steady-state measurements. It has been suggested that PDC renders G$\beta\gamma$ soluble by opening a binding pocket in the Gβ propeller that engulfs the prenyl group attached to Gγ (Lukov et al., 2004). Thus, the long term effects of PDC and PDCL may use such a mechanism to prevent the re-association of G$\beta\gamma$ with Gα, although our data do not specifically address this mechanism. The effects of PDC and PDCL on direct activation of G-proteins (Fig. 6) rule out receptor desensitization as the sole mechanism for these effects.

A second goal of these studies was to evaluate potential roles for PDCL in modulating G-protein mediated ion channel modulation. Western blot analysis indicated that PDCL, but not PDC, is expressed in sympathetic ganglia (Fig. 4) consistent with the ubiquitous expression pattern of the former and more restricted expression pattern (i.e., retina and pineal) of the latter. Although the effects of PDCL expression mimicked those of PDC, recent studies indicate the PDCL is involved in the assembly of Gβ with Gγ (Humrich et al., 2005; Knol et al., 2005; Lukov et al., 2005). Thus, although our results are compatible with the idea that PDCL plays an analogous role in neurons to PDC in the retina, it seems likely that PDCL subserves a more restricted role. For example, small interfering RNA directed against PDCL mRNA reduces G$\beta\gamma$ protein expression (Lukov et al., 2005). Within this context, G$\beta\gamma$ might be expected to be up-regulated when PDCL is overexpressed in SCG neurons. However, the decrease in basal facilitation ratio observed after PDCL expression (Fig. 1) suggests that this does not occur on the time scale of our experiments (~24 h).

Acknowledgments

We thank Dr. Barry M. Willardson (Brigham Young University, Provo, UT) for providing rabbit anti-PDC and anti-(GST)-PDCL polyclonal antibodies and Steven Vogel (National Institutes of Health/National Institute on Alcohol Abuse and Alcoholism) for assistance with the confocal microscopy.

References

Bünemann M, Frank M, and Lohse MJ (2003) Gi protein activation in intact cells involves subunit rearrangement rather than dissociation. *Proc Natl Acad Sci USA* **100:**16077–16082.

Elmslie KS, Zhou W, and Jones SW (1990) LHRH and GTP-γ-S modify calcium current activation in bullfrog sympathetic neurons. *Neuron* **1:**75–80.

Ford CE, Skiba NP, Bae H, Daaka Y, Reuveny E, Shekter LR, Rosal R, Weng G, Yang CS, Iyengar R, et al. (1998) Molecular basis for interactions of G protein $\beta\gamma$ subunits with effectors. *Science (Wash DC)* **280:**1271–1274.

Garcia DE, Li B, Garcia-Ferreiro RE, Hernandez-Ochoa EO, Yan K, Gautam N, Catterall WA, Mackie K, and Hille B (1998) G-protein β-subunit specificity in the fast membrane-delimited inhibition of Ca^{2+} channels. *J Neurosci* **18:**9163–9170.

Gaudet R, Bohm A, and Sigler PB (1996) Crystal structure at 2.4 Å resolution of the complex of transducin $\beta\gamma$ and its regulator, phosducin. *Cell* **87:**577–588.

Gaudet R, Savage JR, McLaughlin JN, Willardson BM, and Sigler PB (1999) A molecular mechanism for the phosphorylation-dependent regulation of heterotrimeric G proteins by phosducin. *Mol Cell* **3:**649–660.

Hu CD and Kerpolla TK (2003) Simultaneous visualization of multiple protein interactions in living cells using multicolor fluorescence complementation analysis. *Nat Biotechnol* **21:**539–545.

Humrich J, Bermel C, Grubel T, Quitterer U, and Lohse MJ (2003) Regulation of phosducin-like protein by casein kinase 2 and N-terminal splicing. *J Biol Chem* **278:**4474–4481.

Humrich J, Bermel C, Bünemann M, Harmark L, Frost R, Quitterer U, and Lohse MJ (2005) Phosducin-like protein regulates G-protein $\beta\gamma$ folding by interaction with tailless complex polypeptide-1α. *J Biol Chem* **280:**20042–20050.

Ikeda SR (1991) Double-pulse calcium channel current facilitation in adult rat sympathetic neurons. *J Physiol* **439:**181–214.

Ikeda SR (1996) Voltage-dependent modulation of N-type calcium channels by G-protein $\beta\gamma$ subunits. *Nature (Lond)* **380:**255–258.

Ikeda SR (2004) Expression of G-protein signaling components in adult mammalian neurons by microinjection. *Methods Mol Biol* **259:**167–181.

Jarvis SE and Zamponi GW (2001) Interactions between presynaptic Ca^{2+} channels, cytoplasmic messengers and proteins of the synaptic vesicle release complex. *Trends Pharmacol Sci* **22:**519–525.

Jeong SW and Ikeda SR (1999) Sequestration of G-protein $\beta\gamma$ subunits by different G-protein α subunits blocks voltage-dependent modulation of Ca^{2+} channels in rat sympathetic neurons. *J Neurosci* **19:**4755–4761.

Kammermeier PJ and Ikeda SR (1999) Expression of RGS2 alters the coupling of metabotropic glutamate receptor 1a to M-type K^+ and N-type Ca^{2+} channels. *Neuron* **22:**819–829.

Kammermeier PJ, Davis MI, and Ikeda SR (2003) Specificity of metabotropic glutamate receptor 2 coupling to G proteins. *Mol Pharmacol* **63:**183–191.

Knol JC, Engel R, Blaauw M, Visser AJ, and van Haastert PJ (2005) The phosducin-like protein PhLP1 is essential for G$\beta\gamma$ dimer formation in Dictyostelium discoideum. *Mol Cell Biol* **25:**8393–8400.

Laemmli UK (1970) Cleavage of structural proteins during the assembly of the head of bacteriophage T4. *Nature (Lond)* **227:**680–685.

Lee RH, Lieberman BS, and Lolley RN (1987) A novel complex from bovine visual cells of a 33,000-dalton phosphoprotein with β- and γ-transducin: purification and subunit structure. *Biochemistry* **26:**3983–3990.

Loew A, Ho YK, Blundell T, and Bax B (1998) Phosducin induces a structural change in transducin $\beta\gamma$. *Structure* **6:**1007–1019.

Lukov GL, Hu T, McLaughlin JN, Hamm HE, and Willardson BM (2005) Phosducin-like protein acts as a molecular chaperone for G protein $\beta\gamma$ dimer assembly. *EMBO (Eur Mol Biol Organ) J* **24:**1965–1975.

Lukov GL, Myung CS, McIntire WE, Shao J, Zimmerman SS, Garrison JC, and Willardson BM (2004) Role of the isoprenyl pocket of the G protein $\beta\gamma$ subunit complex in the binding of phosducin and phosducin-like protein. *Biochemistry* **43:**5651–5660.

Miles MF, Barhite S, Sganga M, and Elliott M (1993) Phosducin-like protein: an ethanol-responsive potential modulator of guanine nucleotide-binding protein function. *Proc Natl Acad Sci USA* **90:**10831–10835.

Miyawaki (2003) A visualization of the spatial and temporal dynamics of intracellular signaling. *Dev Cell* **4:**295–305.

Müller S, Straub A, Schröder S, Bauer PH, and Lohse MJ (1996) Interactions of phosducin with defined G protein $\beta\gamma$-subunits. *J Biol Chem* **271:**11781–11786.

Nagai T, Sawano A, Park ES, and Miyawaki A (2001) Circularly permuted green fluorescent proteins engineered to sense Ca^{2+}. *Proc Natl Acad Sci USA* **98:**3197–3202.

Rishal I, Porozov Y, Yakubovich D, Varon D, and Dascal N (2005) G$\beta\gamma$-dependent and G$\beta\gamma$-independent basal activity of G protein-activated K^+ channels. *J Biol Chem* **280:**16685–16694.

Savage JR, McLaughlin JN, Skiba NP, Hamm HE, and Willardson BM (2000) Functional roles of the two domains of phosducin and phosducin like-protein. *J Biol Chem* **275:**30399–30407.

Schofield GG (1991) Norepinephrine inhibits a Ca^{2+} current in rat sympathetic neurons via a G-protein. *Eur J Pharmacol* **207:**195–207.

Schröder S and Lohse MJ (1996) Inhibition of G-protein $\beta\gamma$-subunit functions by phosducin-like protein. *Proc Natl Acad Sci USA* **93:**2100–2104.

Schröder S and Lohse MJ (2000) Quantification of the tissue levels and function of the G-protein regulator phosducin-like protein (PhlP). *Naunyn-Schmiedeberg's Arch Pharmacol* **362:**435–439.

Schulz R (2001) The pharmacology of phosducin. *Pharmacol Res* **43:**1–10.

Schulz R, Schulz K, Wehmeyer A, and Murphy J (1998) Translocation of phosducin in living neuroblastoma x glioma hybrid cells (NG108–15) monitored by red-shifted green fluorescent protein. *Brain Res* **790:**347–356.

Sokolov M, Strissel KJ, Leskov IB, Michaud NA, Govardovskii VI, and Arshavsky VY (2004) Phosducin facilitates light-driven transducin translocation in rod photoreceptors. Evidence from the phosducin knockout mouse. *J Biol Chem* **279:**19149–19156.

Thibault C, Sganga MW, and Miles MF (1997) Interaction of phosducin-like protein with G protein $\beta\gamma$ subunits. *J Biol Chem* **272:**12253–12256.

Thulin CD, Howes K, Driscoll CD, Savage JR, Rand TA, Baehr W, and Willardson BM (1999) The immunolocalization and divergent roles of phosducin and phosducin-like protein in the retina. *Mol Vis* **29:**40–50.

Thulin CD, Savage JR, McLaughlin JN, Truscott SM, Old WM, Ahn NG, Resing KA, Hamm HE, Bitensky MW, and Willardson BM (2001) Modulation of the G protein regulator phosducin by Ca^{2+}/calmodulin-dependent protein kinase II phosphorylation and 14-3-3 protein binding. *J Biol Chem* **276:**23805–23815.

Xu J, Wu D, Slepak VZ, and Simon MI (1995) The N terminus of phosducin is involved in binding of $\beta\gamma$ subunits of G protein. *Proc Natl Acad Sci USA* **92:**2086–2090.

Address correspondence to: Dr. Stephen R Ikeda, Laboratory of Molecular Physiology, NIH/NIAAA/DICBR, 5625 Fishers Lane, Room TS11A, MSC 9411, Bethesda, MD 20892-9411. E-mail: sikeda@mail.nih.gov